Journal of Medicinal Chemistry

Article

pubs.acs.org/jmc

Novel HldE-K Inhibitors Leading to Attenuated Gram Negative Bacterial Virulence

Nicolas Desroy,[†,∥] Alexis Denis,[†,⊥] Chrystelle Oliveira,[†] Dmytro Atamanyuk,[†] Sophia Briet,[†] Fabien Faivre,[†] Géraldine LeFralliec,[†] Yannick Bonvin,[†] Mayalen Oxoby,[†] Sonia Escaich,[‡,#] Stéphanie Floquet,[‡] Elodie Drocourt,[‡] Vanida Vongsouthi,[‡] Lionel Durant,[‡,∞] François Moreau,[‡] Theodore B. Verhey,[§] Ting-Wai Lee,[§] Murray S. Junop,[§] and Vincent Gerusz*[,†]

[†]Medicinal Chemistry and [‡]Biology, Mutabilis, 102 Avenue Gaston Roussel, 93230 Romainville, France

[§]Department of Biochemistry and Biomedical Sciences and Michael G. DeGroote Institute for Infectious Disease Research, McMaster University, 1280 Main Street West, Hamilton, Ontario, L8S 4K1, Canada

Supporting Information

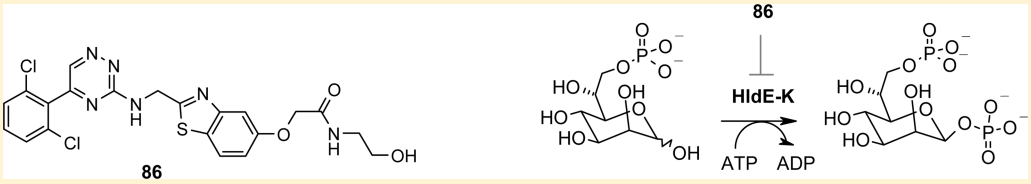

ABSTRACT: We report here the optimization of an HldE kinase inhibitor to low nanomolar potency, which resulted in the identification of the first reported compounds active on selected *E. coli* strains. One of the most interesting candidates, compound **86**, was shown to inhibit specifically bacterial LPS heptosylation on efflux pump deleted *E. coli* strains. This compound did not interfere with *E. coli* bacterial growth (MIC > 32 μg/mL) but sensitized this pathogen to hydrophobic antibiotics like macrolides normally inactive on Gram-negative bacteria. In addition, **86** could sensitize *E. coli* to serum complement killing. These results demonstrate that HldE kinase is a suitable target for drug discovery. They also pave the way toward novel possibilities of treating or preventing bloodstream infections caused by pathogenic Gram negative bacteria by inhibiting specific virulence factors.

INTRODUCTION

During the course of a bacterial infection, virulence factors are responsible for the pathogenicity exhibited toward the host.[1,2] In Gram-negative bacteria, the full outer membrane lipopolysaccharide (LPS) is an important virulence factor, since it confers the prokaryotic cell resistance toward innate immune system components. When LPS lacks the inner core oligosaccharide heptoses, the bacteria produce a so-called deep-rough phenotype involving a truncated or "Re-LPS". They are still viable and capable of gut colonization; however, they are unable to mount a productive infection because of their increased sensitivity toward the bactericidal effect of the host complement.[3,4] Since the heptose synthetic pathway described in Scheme 1 is conserved among Gram negative species and has not been described in eukaryotic cells, it represents an attractive target to attenuate bacterial virulence.[5] In addition, this novel anti-infective approach would not affect the commensal flora and would therefore be less likely to generate resistance in this environment than traditional antimicrobial chemotherapy.[6]

In *Escherichia coli*, HldE constitutes the second enzyme involved in the heptose synthetic pathway. It is a bifunctional cytoplasmic protein comprising both carbohydrate kinase and adenylyltransferase domains.[7] Well conserved among Gram-negative bacteria with the notable exceptions of *Acinetobacter*, *Moraxella*, and *Chlamydia*,[8] HldE shares little similarity with human enzymes (40% at the most with human ribokinase). A few HldE inhibitors have recently been disclosed, although without any reported bacterial data.[9−11] This antivirulence target remains therefore largely unexploited at this time, since there are no drugs on the market or in advanced clinical phases acting via this mode of action.

At Mutabilis, a high-throughput screening campaign led to the discovery of compound **1** as an inhibitor of the kinase activity of HldE (HldE-K) with an IC_{50} of 51 μM (Figure 1). Optimization efforts culminated in compound **2**, displaying an IC_{50} of 0.11 μM on HldE-K.[10] However, no satisfactory antivirulence activity was observed on bacterial strains, even in the absence of efflux-pumps. A second screening campaign led to the identification of compound **3**, another HldE-K hit with an IC_{50} of 6 μM. In contrast to the previous inhibitors **1** and **2**, this new compound is not negatively charged, therefore affording a better potential for penetrating the neutral inner membrane of Gram-negative pathogens. Herein we describe the structure−activity relationship (SAR) of this novel series of compounds active against HldE-K. We also report for the first time specific inhibition of LPS heptosylation on selected *E. coli* strains leading to attenuation of bacterial virulence.

Received: October 16, 2012
Published: February 14, 2013

Scheme 1. Synthesis of ADP-L-*glycero*-β-D-*manno*-heptose from Sedoheptulose 7-Phosphate and Incorporation into LPS in *E. coli*

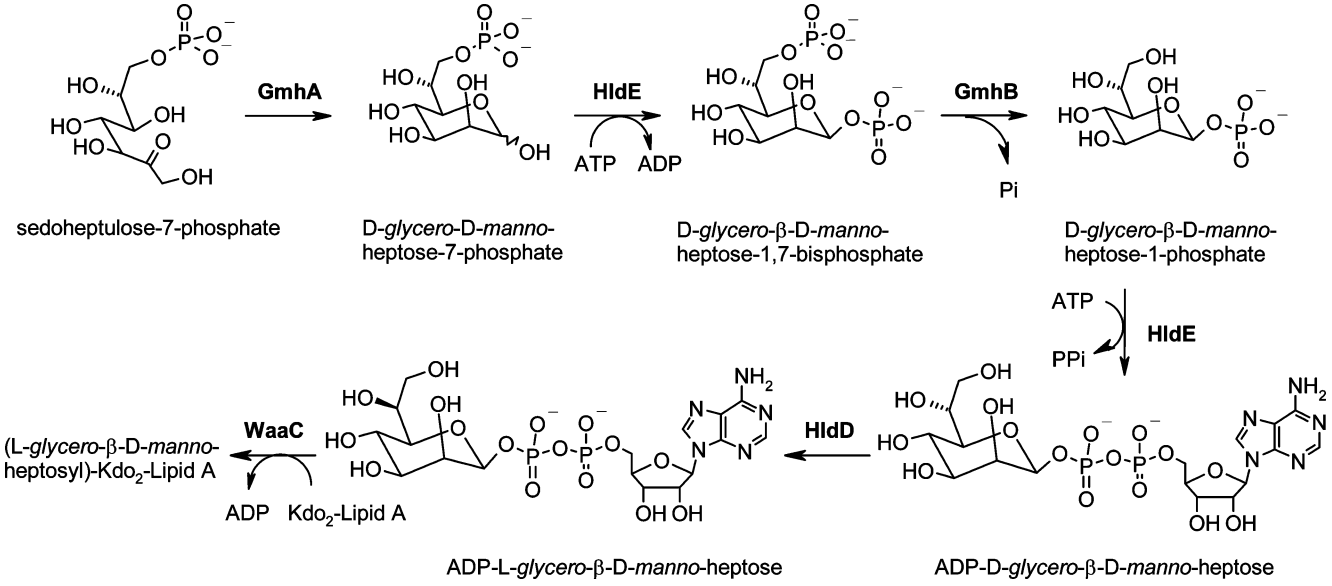

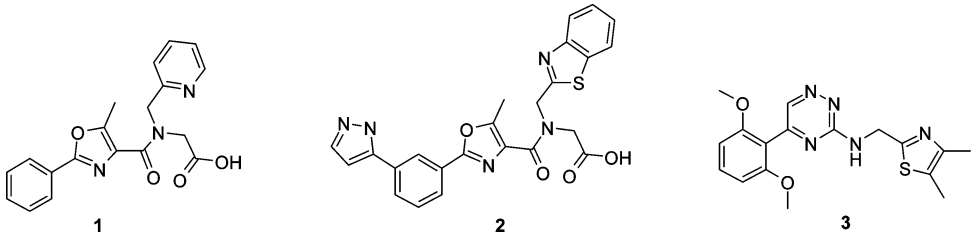

Figure 1. HldE-K inhibitors.

CHEMISTRY

One of the strategies used to synthesize thiazol-2-ylmethylamine analogues began with silylation of thiazole **4** followed by formylation at position 2 and reductive amination, which afforded amine **6** (Scheme 2). Another procedure resorted to the oxidation of available 2-methylbenzothiazoles **7** and **8** by selenium dioxide and subsequent reductive amination to deliver amino intermediates **9** and **10**. 5-Hydroxybenzothiazole derivative **11** was prepared by boron tribromide demethylation of **10**. Palladium-promoted cyclocondensation[12] of **12** with **13** followed by Boc-deprotection under acidic conditions yielded **14**. Replacing **13** by 4-chloro-2-iodoaniline in a similar condensation afforded (6-chloro-1,3-benzothiazol-2-yl)-methylamine used in the preparation of **15**.

One method used to build the triazine template was based on bromination of 1-(2,6-dimethoxyphenyl)ethanone **16** followed by formation of a dimorpholine ketoaminal able to cyclize with aminoguanidine to yield 3-aminotriazine **18** (Scheme 3).[13] A subsequent Sandmeyer reaction afforded 3-chlorotriazine **19**, which served as the building block for nucleophilic substitutions with the corresponding thiazol-2-ylmethylamine derivatives to provide **15**, **20**, **22**, **23**, **26**, and **28**. Compounds **3** and **30**–**48** (Tables 1 and 2) and precursors of **49** (Table 1) and **50** (Table 2) were obtained in similar conditions using appropriate amines, either commercially or synthesized according to known procedures.[14] Compound **51** (Table 1) was prepared similarly from **19** and **6** after acid-mediated deprotection of its silylated precursor. Saponification of **20**

Scheme 2. Preparation of Thiazol-2-ylmethylamine Building Blocks[a]

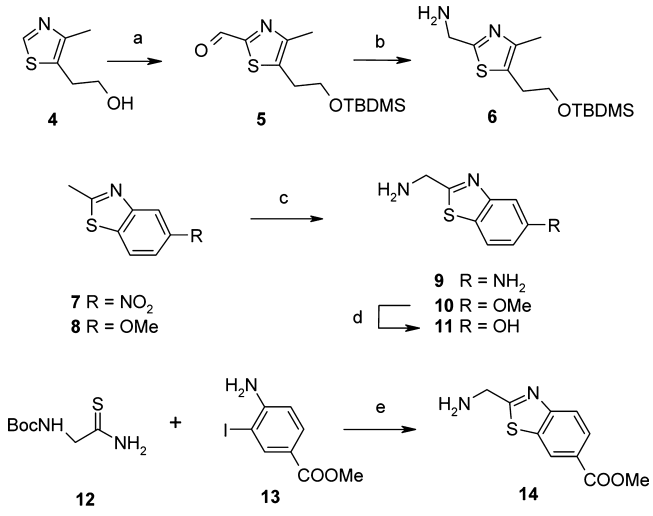

[a]Reagents and conditions: (a) (i) TBDMSCl, imidazole, CH_2Cl_2, rt; (ii) *n*-BuLi, DMF, THF, −78 to −15 °C, 67% over two steps; (b) (i) $H_2NOH{\cdot}HCl$, MeONa, EtOH, rt; (ii) Zn, AcOH, 0 °C to rt, 91% over two steps; (c) (i) SeO_2, 1,4-dioxane, 105 °C; (ii) $H_2NOH{\cdot}HCl$, MeONa, EtOH, rt; (iii) Zn, AcOH, rt, 42% over three steps; (d) BBr_3, DCM, −78 °C to rt, 37%; (e) (i) $Pd_2(dba)_3$, dppf, CaO, acetonitrile, 60 °C; (ii) HCl (37% aq), EtOAc, 0 °C, 16% over two steps.

dx.doi.org/10.1021/jm301499r | J. Med. Chem. 2013, 56, 1418−1430

Scheme 3. Synthesis of Compounds Represented in Tables 1 and 2[a]

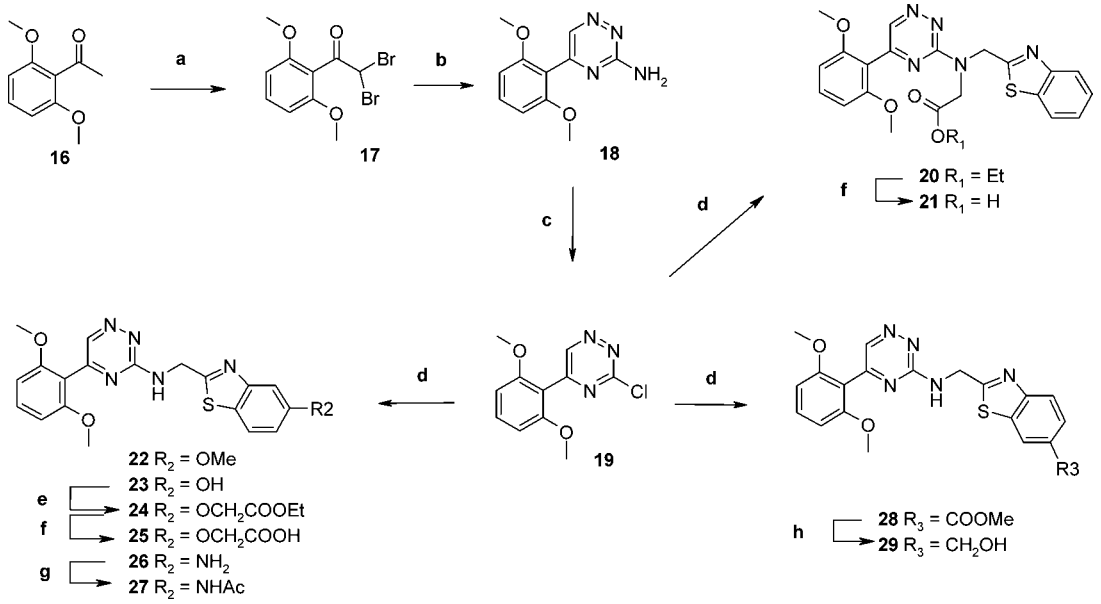

[a]Reagents and conditions: (a) phenyltrimethylammonium tribromide, THF, rt, 86%; (b) (i) morpholine, THF, 67 °C; (ii) aminoguanidine bicarbonate, MeOH, AcOH, 67 °C, 31% over two steps; (c) *t*-BuONO, $CuCl_2$, ACN, DCM, 65 °C, 29%. (d) For **20**: ethyl [(1,3-benzothiazol-2-ylmethyl)amino]acetate,[14] DIPEA, ACN, 80 °C, 8%. For **22**: **10**, DIPEA, ACN, 80 °C, 72%. For **23**: **11**, ACN, 85 °C, 70%. For **26**: **9**, ACN, 85 °C, 46%. For **28**: **14**, DIPEA, ACN, 80 °C, 43%. (e) $BrCH_2COOEt$, K_2CO_3, THF, 50 °C, 27%; (f) LiOH, THF, H_2O, rt. For **21**: 44%. For **25**: 65%. (g) AcCl, pyridine, DCM, 0 °C, 32%; (h) DIBAL-H (1 M in toluene), DCM, −78 to −45 °C, 48%.

afforded **21**, and compound **49** was obtained likewise. Alkylation of **23** with ethyl bromoacetate followed by hydrolysis under basic conditions afforded **25**. Acetylation of **26** provided **27**, while a similar reaction on the amino derivative obtained by substitution of **19** with 6-aminobenzothiazolylmethylamine prepared as **9** yielded **50**. Compound **29** was synthesized by DIBAL-H reduction of **28**.

Compounds **54** and **59**−**61** (Table 3) incorporating a nonaromatic left part were prepared according to Scheme 4.

Scheme 4. Synthesis of 5-(Alkyl/piperazinyl)-1,2,4-triazine Derivatives Represented in Table 3[a]

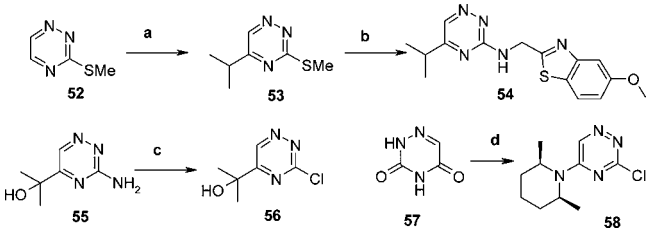

[a]Reagents and conditions: (a) (i) *i*-PrLi (0.7 M in pentane), THF, −78 °C; (ii) DDQ, toluene, rt, 26% over two steps; (b) (i) mCPBA, DCM, rt; (ii) **10**, DIPEA, ACN, 85 °C, 14% over two steps; (c) *t*-BuONO, $CuCl_2$, acetonitrile, 70 °C, 41%; (d) (i) $POCl_3$, TEA, dioxane, 110 °C; (ii) *cis*-2,6-dimethylpiperidine, ACN, 0 °C, 3% over two steps.

Isopropyllithium addition at position 5 of triazine **52** with subsequent 2,3-dichloro-5,6-dicyano-1,4-benzoquinone oxidation afforded **53**. Thioether oxidation followed by substitution with amine **10** under basic conditions yielded **54**. Chlorotriazine **56** was prepared by Sandmeyer chlorination of intermediate **55**[15] and was then transformed to **59** under previously described substitution conditions with **10**. Chlorination of 6-azauracil[16] followed by subsequent substitution with *cis*-2,6-dimethylpiperidine afforded **58**, which was transformed into **60** under classical conditions with **10**. Compound **61** was obtained in the same manner as **60**, using 6-azauracil and 2-piperidinemethanol.

The preparation of some 5-aryl-1,2,4-triazine derivatives involved another pathway using selenium dioxide oxidation of acetophenones to glyoxal intermediates followed by cyclocondensation with thiosemicarbazide (Scheme 5).[17] In this manner, 1-(2-methoxynaphthalen-1-yl)ethanone **62**[18] was transformed into triazin-3-ol, which was submitted to chloration of position 3 with phosphoryl chloride to provide **63**. Substitution under standard conditions with amine **10** afforded **64**. Compounds **66** and **72**−**75** (Table 3) were obtained similarly. Demethylation of **64** under boron tribromide conditions yielded **65**. The same procedure was used to obtain **76**. The meta-position of the left-part aryl group of **66** was modified under palladium-catalyzed conditions: triethylsilane reduction of the meta-bromide moiety yielded **67**, while Buchwald coupling with acetamide afforded **68** and Suzuki coupling with the corresponding boronic acids provided **69** and **77** (Table 3). In a similar way, **74** was transformed to **78**−**80** (Table 3). Compound **70**, which was prepared by standard substitution of the corresponding chlorotriazine[14] with **10**, was reacted under basic conditions with 2-chloro-*N*,*N*-dimethylethanamine to afford **71**.

The synthesis of the compounds represented in Table 4 is illustrated in Scheme 6. O-Alkylation of **81**, obtained by standard demethylation of **72**, afforded derivatives **82** and **83**. Reduction of ester **83** under hydride conditions provided alcohol **84**, while its hydrolysis with lithium hydroxide led to carboxylic acid **85** that was derivatized to amides **86** and **95** (Table 4) under classical peptide coupling conditions. Phthalimide protection of **10** followed by demethylation with boron tribromide yielded intermediate **88**, which was O-

dx.doi.org/10.1021/jm301499r | *J. Med. Chem.* 2013, 56, 1418−1430

Scheme 5. Synthesis of 5-Aryl-1,2,4-triazine Derivatives Represented in Table 3[a]

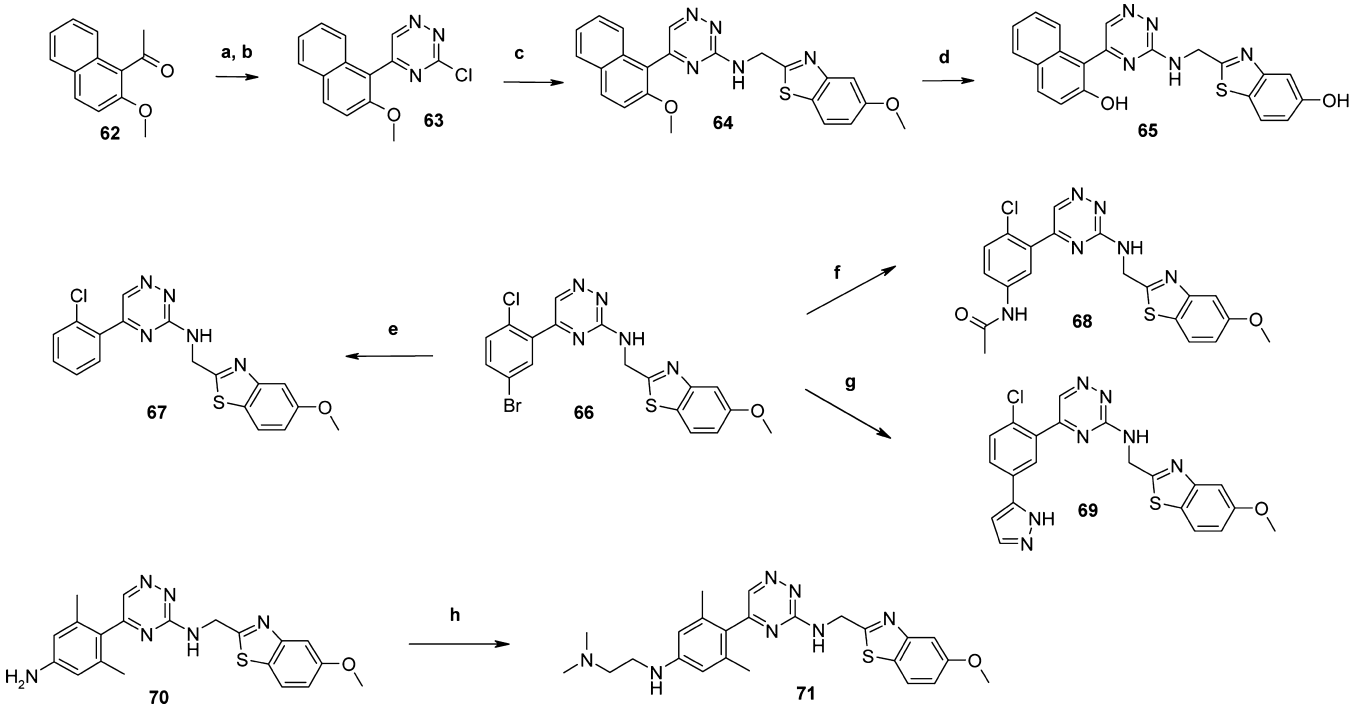

[a]Reagents and conditions: (a) (i) SeO_2, dioxane, H_2O, 105 °C; (ii) semicarbazide·HCl, K_2CO_3, EtOH·H_2O, 105 °C, 30% over two steps; (b) $POCl_3$, DMF, $CHCl_3$, 50 °C, 60%; (c) **10**, DIPEA, ACN, 85 °C, 56%; (d) BBr_3, DCM, −78 °C to rt, 65%; (e) triethylsilane, $PdCl_2(dppf)_2$·DCM, CsF, 1,4-dioxane, 19%; (f) CH_3CONH_2, CsF, xantphos, $Pd_2(dba)_3$, 1,4-dioxane, 100 °C, 14%; (g) 1*H*-pyrazol-3-ylboronic acid, Na_2CO_3, $Pd(PPh_3)_4$, DMF, 100 °C, 51%; (h) 2-chloro-*N*,*N*-dimethylethanamine hydrochloride, $NaHCO_3$, NaI, BuOH, 110 °C, 27%.

alkylated with *N*-(2-chloroethyl)-*N*,*N*-dimethylamine, deprotected with methylhydrazine, and substituted with 3-chloro-5-(2,6-dichlorophenyl)-1,2,4-triazine to provide **90**. Intermediate **88** was also submitted to Mitsunobu conditions with *tert*-butyl 2-hydroxyethylcarbamate to afford after phthalimide deprotection amine **91**, which was substituted with 3-chloro-5-(2,6-dichlorophenyl)-1,2,4-triazine and deprotected under acidic conditions to afford **92**. Acylation of this amine under classical peptide coupling conditions provided compounds **93** and **94** (Table 4).

RESULTS AND DISCUSSION

Optimization of compound **3** was initiated using classical SAR-driven medicinal chemistry approaches to increase HldE-K potency. Later in the project, the procurement of cocrystal structures of some of these inhibitors with HldA of *Burkholderia cenocepacia*, the homologous kinase sharing 49% sequence identity and 62% sequence similarity with *E. coli* HldE-K, allowed some rationalization of our results.[19]

To assess the importance of the 1,2,4-triazine template, a number of other heterocyclic scaffolds were initially synthesized (Figure 2). Since all of these rescaffolding attempts led to a 5- to 20-fold loss of potency against HldE-K (data not shown), the 1,2,4-triazine core was maintained for further exploration.

Various right-part groups were then evaluated to establish SAR in this area (Table 1). Replacing the thiazolyl group by a furanyl moiety led to a complete loss of potency, while the pyrazolyl analogue exhibited a 4-fold loss of potency (**30** and **31** vs **3**). This might suggest the importance of a hydrogen-bond acceptor nitrogen in the right-part heterocycle, which was subsequently confirmed by cocrystal structures.[19] Substituents with hydrogen-bond acceptors or donors at position 5 of the thiazole moiety (**32** and **51**) were found detrimental to potency, suggesting either a steric hindrance or a lipophilic environment in this area. Cyclization of the two methyl groups in benzothiazole or tetrahydrobenzothiazole substituents (**34** and **35**) afforded a 3-fold improvement in potency, confirming the beneficial effect of lipophilic groups in this location. Variation of the orientation of the hydrogen-bond acceptor nitrogen such as in pyridyl **33** or quinolyl **36** or removal of this hydrogen-bond acceptor in benzothiophenyl **37** resulted in a complete loss of potency. Increasing the hydrophilic character of the bicycle such as in benzoxazolyl **38** and in benzimidazolyl **39** or increasing the steric hindrance in 1-methyl-2-benzimidazolyl **40** also proved detrimental. Replacing the nitrogen-containing amine within the linker by an oxygen-containing ether (**41**) led to a 7-fold loss in potency. Introducing a short substituent to this nitrogen was tolerated (**42** vs **3** and **21** vs **34**), although increasing its size proved detrimental (**49** and **43**). Substitutions on the methylene linker bridging the amine and the heterocycle also led to a decrease in potency (**44** and **45**).

The mechanism of action of compound **34** was investigated in order to rule out promiscuous inhibition.[20] Inhibition kinetics of **34** were linear and were not dependent on the order of reagent addition or on enzyme/inhibitor preincubation. The inhibition was also unaltered by Triton-X100 (100 μM to 1 mM) or D-*manno*-heptose 7-phosphate substrate (up to 15 k*m*). Finally, as shown in Figure 3, compound **34** behaved as a competitive reversible inhibitor with respect to ATP (K_i = 2.5 μM). These data suggest that the inhibition specifically takes place in the nucleotide-binding site, which was further substantiated by the cocrystal structures of *B. cenocepacia* HldA with two of the analogues from this series.[19]

dx.doi.org/10.1021/jm301499r | *J. Med. Chem.* 2013, 56, 1418−1430

Scheme 6. Synthesis of Compounds Represented in Table 4[a]

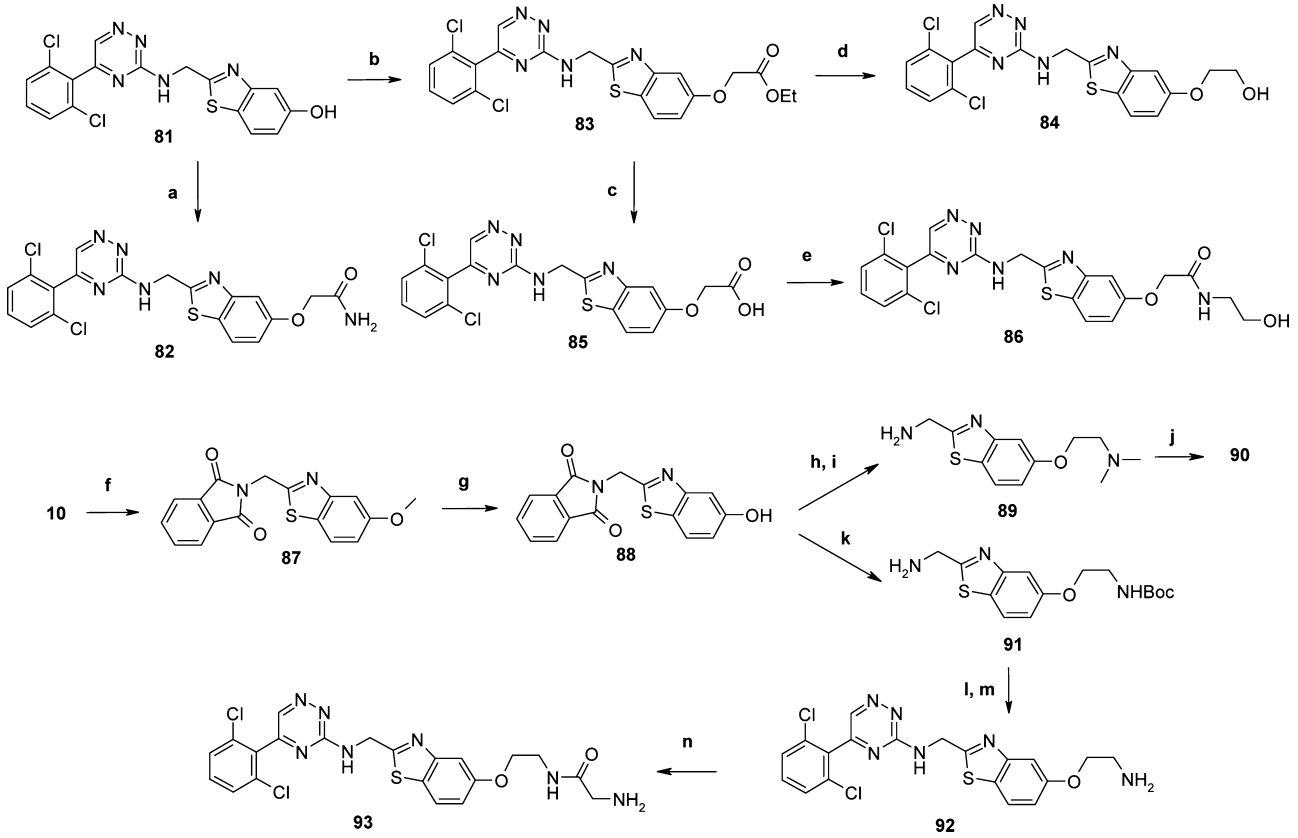

[a]Reagents and conditions: (a) iodoacetamide, K_2CO_3, THF, 50 °C, 40%; (b) ethyl bromoacetate, K_2CO_3, acetone, 60 °C, 43%; (c) LiOH, THF, H_2O, rt, 77%; (d) DIBAL-H, DCM −78 to −30 °C, then $NaBH_4$, MeOH, rt, 52%; (e) ethanolamine, EDAC, 4-DMAP, THF, DCM, rt, 31%; (f) phthalic anhydride, DIPEA, pTSA, toluene, 70 °C, 69%; (g) BBr_3, DCM, −78 °C to rt, 87%; (h) *N*-(2-chloroethyl)-*N*,*N*-dimethylamine·HCl, K_2CO_3, acetone, 60 °C, 56%; (i) $MeNHNH_2$, ethanol, 80 °C, 34%; (j) 3-chloro-5-(2,6-dichlorophenyl)-1,2,4-triazine, DIPEA, ACN, 85 °C; 31%; (k) (i) *tert*-butyl 2-hydroxyethylcarbamate, DIAD, PPh_3, THF, 0 °C to rt, 62%; (ii) $MeNHNH_2$, EtOH, 80 °C, 62%; (l) 3-chloro-5-(2,6-dichlorophenyl)-1,2,4-triazine, DIPEA, ACN, 85 °C; 49%; (m) HCl (4 N in dioxane), MeOH, 0 °C to rt, 58%; (n) (i) $BocNHCH_2COOH$, EDAC, 4-DMAP, THF, DCM, 50 °C; (ii) HCl (4 M in dioxane), THF, MeOH, 0 °C to rt, 7% over two steps.

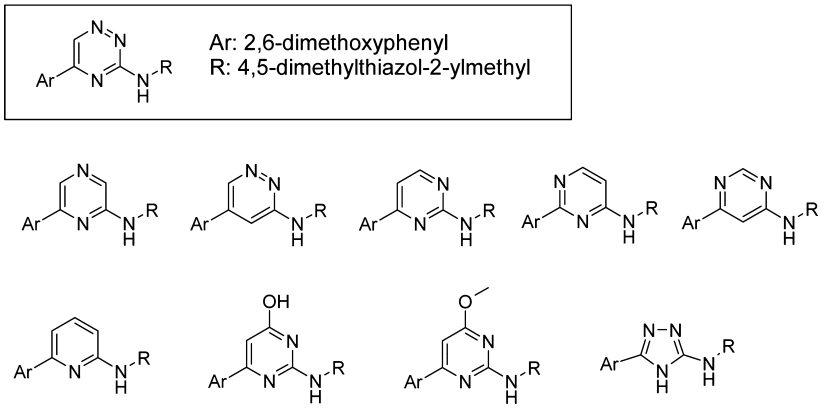

Figure 2. Central rescaffolding of **3**.

Having determined a 3-fold improvement in potency afforded by benzothiazole **34** over the initial hit **3**, we set out to study its substitution potential (Table 2). A variety of different groups were tolerated at position 5, either lipophilic (**46**, **47**, and **22**) or hydrophilic (**23** and **25**−**27**). The most potent compounds **23** and **25** were 5−8 times more active than the unsubstituted benzothiazole **34**. This could be rationalized by a hydrogen bond between the hydroxyl substituent of **23** and the side chain amide group of a conserved asparagine (Asn202 in *B. cenocepacia* HldA and Asn196 in *E. coli* HldE-K). Similarly, the cocrystal structure of *B. cenocepacia* HldA with **25** displays a favorable dipole−dipole interaction between its benzothiazole carboxyl substituent and the side chain amide group of the same conserved asparagine.[19] Position 6 of benzothiazole was less permissive, since groups bulkier than hydroxyl were detrimental to potency (**28**, **29**, **50** vs **48**).

dx.doi.org/10.1021/jm301499r | *J. Med. Chem.* 2013, 56, 1418−1430

Table 1. Influence of the Right-Part Substitution on *E. coli* HldE-K Inhibition

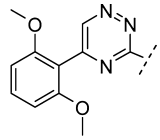

Compd	Right-part	IC_{50} (μM)	Compd	Right-part	IC_{50} (μM)
3	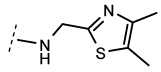	6	**38**	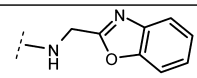	34
30	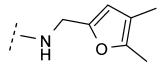	>300	**39**	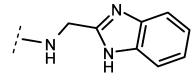	>300
31	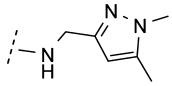	25	**40**	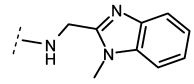	>300
32	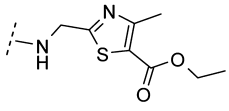	>300	**41**	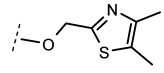	40
51	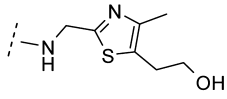	>300	**42**	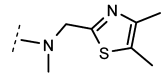	5
33	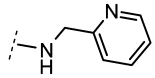	>300	**21**	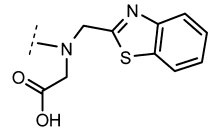	2
34	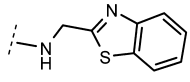	2	**49**	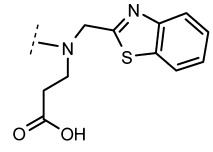	46
35	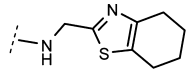	1.9	**43**	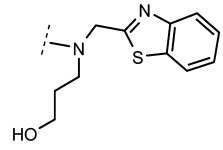	>300
36	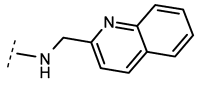	>300	**44**	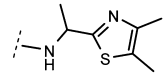	54
37	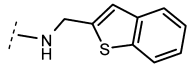	>300	**45**	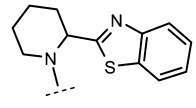	>300

The left-part substitution was then investigated with 5-(methoxy or hydroxy)benzothiazole as the right-part moiety (Table 3). Alkyl groups (**54** and **59**) and nonaromatic heterocycles (**60** and **61**) were inactive, reflecting the importance of an aromatic moiety in this location. Of all the aromatic groups evaluated, the naphthyl derivatives **64** and **65** proved the most active against the enzyme, reaching low nanomolar potency. This suggests a significant π-stacking contribution, supported by the proximity between the benzothiazole and the left-part aromatic groups in the bent inhibitor conformation observed within the cocrystal structures.[19] High-throughput screening of the analogues of our hit revealed that the aromatic group had to be ortho-substituted in order to be active against the enzyme. An ortho, ortho prime substitution is even more beneficial as shown by the 10-fold gain in potency by dichloro-substituted **72** versus monochloro-substituted **67**. The ortho substitution adjusts the left-part aromatic moiety in a perpendicular way to the triazine core,

dx.doi.org/10.1021/jm301499r | *J. Med. Chem.* 2013, 56, 1418−1430

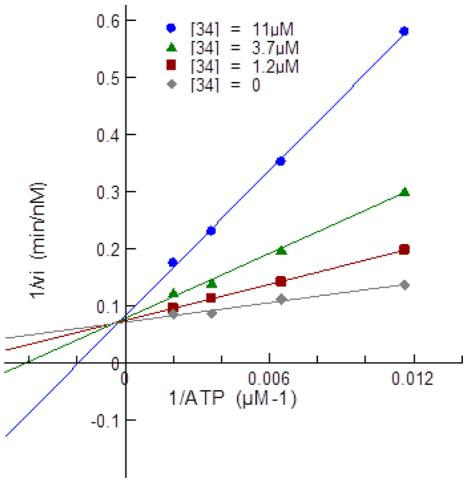

Figure 3. Competition between **34** and ATP for *E. coli* HldE-K measured in the presence of 2 μM of the D-*manno*-heptose 7-phosphate substrate. This double reciprocal plot (1/(initial velocity) vs 1/[ATP]) displays lines intersecting with the vertical axis at $1/V_{max}$.

which could facilitate the π-stacking or Cl–π interactions[21] between the left and right aromatic groups of the compound. Substitutions at the meta position of the left-part phenyl group with both hydrogen-bond donor (**68** and **69**) and acceptor (**77**) are tolerated. The para position also proved permissive, with a variety of substituents allowed (**70**, **71**, **74**, **75**, **79**, and **80**). Cocrystal structures revealed an expansion of the nucleotide-binding site of the enzyme in these directions, which probably accounts for the observed permissiveness of the meta and para substitutions.

The key points of our potency SAR for this series are summarized in Figure 4 and were found to be in full agreement with the previously reported cocrystal structures in *B. cenocepacia* HldA.[19] The triazine scaffold turned out to be optimal, which may be accounted for by H-bonding of N1 and N2 with a canonical water molecule itself bonded to a backbone NH of Leu 258 and possibly a backbone carbonyl of Asn 294. Significant π-stacking or Cl–π interactions between the required left and right aromatic parts of the inhibitors contribute to their folded conformations and improve their shape complementarity with the ADP binding site. The importance of the right-part thiazole nitrogen revealed by our SAR was confirmed by a H-bond interaction with the backbone NH donor group of Ser 240. The highly polar enzymatic environment and the partial solvent exposure at the 5-position of the benzothiazole ring might also account for the relative SAR permissiveness of substitution exhibited at this location.

The discovery of these low nanomolar inhibitors of HldE-K prompted us to investigate their antivirulence effects. Bacteria with heptose-deficient LPS (*hldE*-deleted strains) display increased sensitivity to hydrophobic antibiotics (Table 5), which is possibly due to a reduction in the hydrophilic barrier presented by a Re-LPS versus an intact LPS. We therefore investigated the potential sensitization of efflux-pump deleted strains *E. coli* K12 Δ-*acrAB*, Δ*tolC* and *E. coli* K1 Δ-*tolC* to erythromycin by our inhibitors (Table 6). In both strains, deletion of the major efflux pump AcrAB/TolC (in part or entirely) leads to an increased susceptibility toward amphiphilic and lipophilic antibiotics.[22] The concentration of erythromycin chosen for this study was at one-fourth of its minimal inhibitory concentration (MIC) on these selected strains. The intrinsic antibacterial effects of these compounds were also assessed without erythromycin. In the most promising cases where good sensitization of *E. coli* K1 Δ-*tolC* to erythromycin could be observed without any inhibitor-induced antibacterial effects, further cytotoxicity studies and LPS electrophoresis assays were performed to determine the capacities of those compounds to inhibit specifically the biosynthesis of heptose-containing LPS.

Most of the nanomolar inhibitors in Table 3 were inactive in the sensitization assays. As a notable exception, **65** sensitized *E. coli* K1 Δ-*tolC* to erythromycin at 2 μg/mL (Table 6). However, its intrinsic antibacterial activity against *E. coli* K12 Δ-*acrAB*, Δ-*tolC* and its cytotoxicity on eukaryotic cells cast doubts on a sensitization specifically achieved by heptosylation inhibition, and this compound was therefore not investigated any further.

Since the dichloro derivative **72** exhibited a 5-fold improvement in potency over the dimethoxy derivative **22**, we re-examined the substitutional effects at position 5 of the benzothiazole with the hope of increasing the antibacterial activity (Table 4). As already observed with compounds **23** vs **22**, the replacement of the terminal methoxyl group by a hydroxy group afforded a 1.7-fold gain in potency (**81** vs **72**). Chain extensions with a variety of hydrogen-bond donors and acceptors, whether neutral (**82**, **84**, **86**, and **94**) or charged (**85**, **90**, **92**, **93**, and **95**), were well tolerated with potencies remaining in the nanomolar range. The most potent inhibitors (**84**, **85**, and **95**) have neutral or negatively charged moieties, which may interact favorably with the side chain amide group of the conserved binding pocket asparagine of the enzyme. By contrast, positively charged moieties as found in **90**, **92**, or **93** presented a 5- to 10-fold loss in potency. Despite their good

Table 2. Influence of Benzothiazole Substitution on *E. coli* HldE-K Inhibition

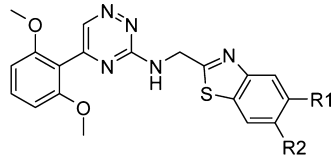

compd	R1	R2	IC_{50} (μM)	compd	R1	R2	IC_{50} (μM)
46	Me	H	1.5	**27**	NHAc	H	7.6
47	Cl	H	1.6	**15**	H	Cl	27
22	OMe	H	0.67	**28**	H	CO_2Me	89
23	OH	H	0.39	**29**	H	CH_2OH	15
25	OCH_2CO_2H	H	0.25	**48**	H	OH	3.4
26	NH_2	H	1.4	**50**	H	NHAc	49

dx.doi.org/10.1021/jm301499r | J. Med. Chem. 2013, 56, 1418–1430

Table 3. Influence of the Left-Part Substitution on *E. coli* HldE-K Inhibition

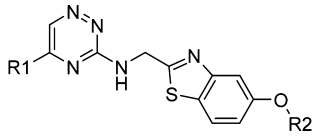

Compd	R1	R2	IC_{50} (μM)	Compd	R1	R2	IC_{50} (μM)
54		Me	>300	**76**		Me	0.069
59		Me	>300	**66**	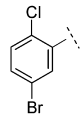	Me	0.760
60		Me	>300	**68**	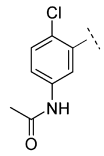	Me	1.4
61	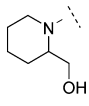	Me	>300	**69**	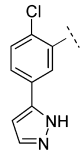	Me	0.053
64	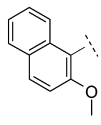	Me	0.051	**77**	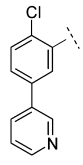	Me	0.150
65	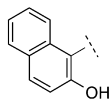	H	0.020	**74**	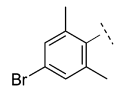	Me	1.2
22	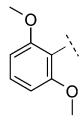	Me	0.670	**75**	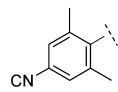	Me	1.4
67		Me	1.4	**70**	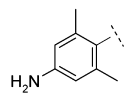	Me	0.320
72		Me	0.130	**79**	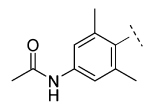	Me	0.240
73		Me	2.4	**80**	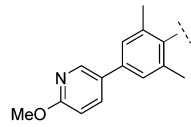	Me	0.890
78		Me	0.360	**71**	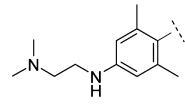	Me	0.082

potency against the enzyme, the negatively charged inhibitors showed poor potency against bacteria (Table 6, **85** and **95**), which might reflect difficulty of these compounds crossing Gram-negative membranes. However, the most potent neutral

dx.doi.org/10.1021/jm301499r | *J. Med. Chem.* 2013, 56, 1418−1430

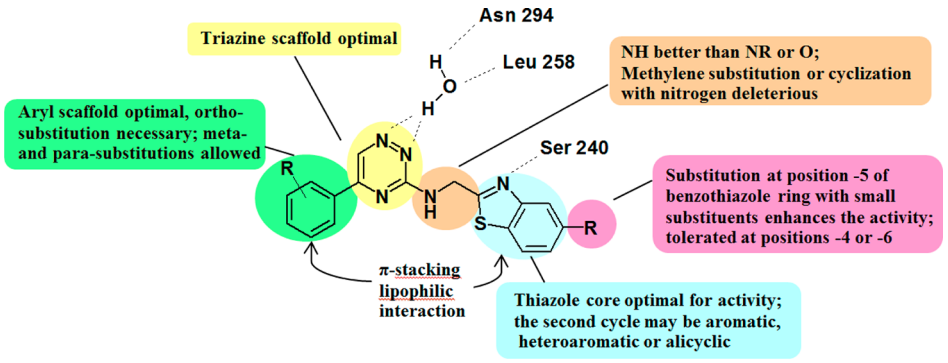

Figure 4. Summary of potency SAR for triazine HldE inhibitors.

Table 4. Influence of 5-Benzothiazolyl Substitution on *E. coli* HldE-K Inhibition

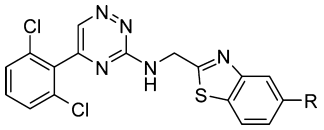

Compd	R	IC_{50} (μM)	Compd	R	IC_{50} (μM)
81	OH	0.075	**90**	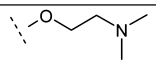	0.082
82	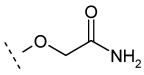	0.067	**95**	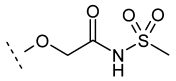	0.016
85	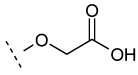	0.019	**86**	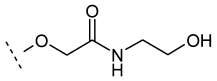	0.049
84	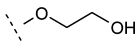	0.018	**94**	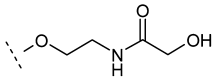	0.071
92	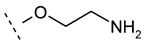	0.185	**93**	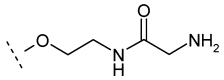	0.100

Table 5. Differential of the MIC in μg/mL between HldE *E. coli* Mutant and Wild Type Strains

	E. coli K1 wild type (μg/mL)	*E. coli* K1 Δ*hldE* (μg/mL)
erythromycin	32	0.5
telithromycin	8	0.25
novobiocin	32	0.5
rifampicin	8	0.125
synercid	>32	2

and positively charged inhibitors (**84**, **86**, **90**, and **93**) displayed for the first time sensitization of *E. coli* K12 Δ-*acrAB*, Δ-*tolC* and K1 Δ-*tolC* strains to erythromycin. Compound **93** was cytotoxic at 18 μg/mL, possibly because of its amphipathic structure, whereas **84** and **90** displayed antibacterial activities at 16−32 μg/mL on *E. coli* K12 Δ-*acrAB*, Δ-*tolC* by themselves. Compound **86** was not by itself antibacterial or cytotoxic at 32 μg/mL but could senzitize K12 Δ-*acrAB*, Δ-*tolC* to erythromycin at 2 μg/mL and K1 Δ-*tolC* to the same antibiotic at 16 μg/mL. These inhibitors were nevertheless unable to senzitize *E. coli* K1 wild-type strain to erythromycin at one-fourth of its MIC (32 μg/mL).

LPS electrophoresis assays were performed with inhibitors alone to determine their capacities in specifically inhibiting the biosynthesis of intact LPS. In this assay, **86** started to inhibit LPS synthesis at 2 μg/mL in *E. coli* K12 Δ-*acrAB*, Δ-*tolC* and at 16 μg/mL in K1 Δ-*tolC* (Figure 5). These concentrations are in line with the ones observed in Table 6 that afforded sensitization effects to erythromycin, thereby demonstrating a specific mode of action. Potential bacterial sensitization to complemented serum by **86** was also assessed (Table 7), since Gram-negative bacteria devoid of heptose-containing LPS are known to be susceptible to the complement system.[3,4] While, as expected, no antibacterial effects were observed against K12 Δ-*acrAB*, Δ-*tolC* in the absence of serum complement, its presence inhibited bacterial growth with 4 μg/mL **86**. This assay provided evidence that our inhibitor attenuated the virulence of this selected Gram-negative strain under simulated physiological conditions through sensitizing bacteria to killing by serum complement.

The ability of these inhibitors to recognize the nucleotide-binding sites of other closely related enzymes was investigated to determine their Gram-negative potential spectra as well as their selectivity (Table 8). Inhibition data for HldE-K enzymes from *K. pneumoniae*, *S. marcescens*, or *N. meningitidis* revealed

dx.doi.org/10.1021/jm301499r | *J. Med. Chem.* 2013, 56, 1418−1430

Table 6. In Vitro Evaluation of Selected Compounds

compd	IC_{50} (μM), *E. coli* HldE-K	MIC (μg/mL), *E. coli* K12 Δ-*acrAB*, Δ-*tolC*		MIC (μg/mL), *E. coli* K1 Δ-*tolC*		cytotoxicity, HepG2 (μg/mL)
		without erythromycin	+1 μg/mL erythromycin[a]	without erythromycin	+1 μg/mL erythromycin[b]	
64	0.051	>32	>32	>32	>32	
65	0.020	2	0.063	>32	2	20
72	0.130	>32	>32	>32	>32	
78	0.360	>32	>32	>32	>32	
76	0.069	>32	8	>32	>32	
69	0.053	>32	>32	>32	>32	
79	0.240	>32	>32	>32	>32	
71	0.082	>32	>32	>32	>32	
81	0.075	>32	>32	>32	>32	
82	0.067	>32	>32	>32	>32	
85	0.019	>32	32	>32	>32	
84	0.018	16	0.5	>32	32	>32
90	0.082	32	4	>32	16	>32
95	0.016	>32	>32	>32	>32	
86	0.049	>32	2	>32	16	>32
94	0.071	>32	4	>32	>32	
93	0.100	32	4	>32	32	18

[a]Erythromycin concentration is at one-fourth of its own MIC against *E. coli* K12 Δ-*acrAB*, Δ-*tolC*. [b]Erythromycin concentration is at one-fourth of its own MIC against *E. coli* K1 Δ-*tolC*.

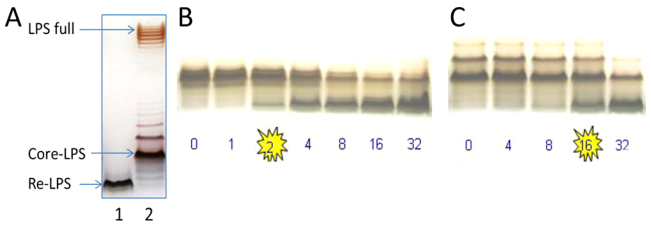

Figure 5. LPS electrophoresis assays. (A) Positive and negative controls obtained with (1) LPS of *E. coli* K1-ΔhldE and (2) LPS of *E. coli* K1 wild type. (B) LPS of *E. coli* K12 Δ-*acrAB*, Δ-*tolC* incubated for 5 h at 37 °C with different concentrations (in μg/mL) of **86**. The highlighted concentration corresponds to the lowest dose at which Re-LPS was observed. (C) LPS of *E. coli* K1 Δ-*tolC* incubated for 5 h at 37 °C with different concentrations (in μg/mL) of **86**. The highlighted concentration corresponds to the lowest dose at which Re-LPS was observed.

Table 7. *E. coli* K12 Δ-*acrAB*, Δ-*tolC* Sensitization to Serum Complement by 86

compd	MIC (μg/mL) against *E. coli* K12 Δ-*acrAB*, Δ-*tolC*		
	no FBS[a]	with 30% of decomplemented FBS[a]	with 30% of normal FBS[a]
86	>32	>32	4

[a]Fetal bovine serum.

good conservation of the SAR observed for *E. coli*. Most potent compounds against *E. coli* HldE-K such as **65**, **85**, or **86** were also low nanomolar inhibitors against the related enzymes from *K. pneumoniae* and *S. marcescens* but displayed a 100-fold decrease in potency against *N. meningitidis* HldE-K. These results indicate the potential for these inhibitors exhibiting broad-spectrum potency against Gram-negative pathogens. The absence of potency against *E. coli* ribokinase, the most sequentially similar nonrelated enzyme of HldE-K (sequence similarity, 38%) at 300 μM, demonstrates the high selectivities of these inhibitors against ribokinase, which is present in both prokaryotes and eukaryotes.

Table 8. Potency against Related Enzymes

compd	IC_{50} (μM)				
	ECO[a] HldE-K	KPN[b] HldE-K	SMA[c] HldE-K	NM[d] HldE-K	ECO[a] RK[e]
76	0.069	0.430	0.160	9.8	>300
72	0.130	2.3	1.2	13	>300
65	0.020	0.085	0.041	1.3	>300
85	0.019	0.100	0.041	1.8	>300
86	0.049	0.150	0.076	1.9	>300

[a]ECO: *E. coli*. [b]KPN: *Klebsiella pneumoniae*. [c]SMA: *Serratia marcescens*. [d]*Neisseria meningitidis*. [e]Ribokinase.

CONCLUSION

We report here the optimization of an HldE-K inhibitor resulting in the development of several compounds with low nanomolar potency against this necessary LPS biosynthetic enzyme. This study resulted in the identification of the first HldE-K inhibitors active against selected *E. coli* strains. One of the most interesting candidates, compound **86**, was shown to attenuate Gram-negative bacterial virulence with a specific mode of action, without displaying intrinsic antibacterial activity. By inhibiting LPS biosynthesis of *E. coli* K12 Δ-*acrAB*, Δ-*tolC*, **86** could sensitize this strain to killing by serum complement under simulated physiological conditions. Selectivity and the potential for acting against a broad Gram-negative spectrum were also demonstrated for this series of compounds. These results pave the way toward novel possibilities of treating or preventing bloodstream infections caused by pathogenic Gram negative bacteria without affecting their commensal flora, thus exerting potentially less selective pressure for antibiotic resistance than conventional antibacterial chemotherapy. The recently determined cocrystal structures of two of these inhibitors with HldA of *B. cenocepacia* represent an attractive perspective for further optimizing their inhibitory potential on wild-type bacterial strains. Some subsequent developments are reported in a following article.[23]

dx.doi.org/10.1021/jm301499r | *J. Med. Chem.* 2013, 56, 1418−1430

EXPERIMENTAL SECTION

Plasmid Construction, Expression, and Purification of HldE and RK. Genes encoding HldE were amplified by PCR from the genomic DNA of *E. coli* O18:K1 C7 (Robert Debré Hospital, Paris), *N. meningitidis* 2C43 (Necker Hospital, Paris), *S. marcescens* NEM017811 (Necker Hospital, Paris), and *K. pneumoniae* ATCC700603 (LGC Promochem) by using Pfu polymerase (Promega). Similarly, a gene encoding ribokinase was amplified from *E. coli* K12 MG1655 (Robert Debré Hospital, Paris). PCR fragments were cloned into pET101 (except for *hldE* of *E. coli*: pET100) expression vector (Invitrogen), and the resulting plasmids were used to transform *E. coli* Top10 (Invitrogen). Finally, purified plasmids were used to transform *E. coli* BL21 (Invitrogen). Nucleotide sequencing of the various cloned fragments revealed no mutation. Recombinant proteins were expressed and purified as described: Exponential-phase culture (optical density at 600 nm, 0.5−0.7) was induced for expression by the addition of isopropyl-β-D-glucopyranoside (IPTG) at a final concentration of 0.5 mM and incubated for further 3 h. Bacterial cells containing overexpressed recombinant proteins were harvested by centrifugation, and cell lysis was performed by sonication. After the removal of cell debris or unlysed cells by centrifugation, Ni-NTA agarose (Sigma) was added to the supernatant (i.e., soluble fraction). Binding of the recombinant protein with the gel matrix was maximized by incubation at 4 °C. His-tagged proteins were eluted by stepwise increasing concentrations of imidazole (Sigma). The various fractions were analyzed by SDS−PAGE, and fractions containing the recombinant protein were pooled and concentrated by ultrafiltration (Amicon Ultra-15-Millipore). Protein concentration was determined by Bradford Method (Invitrogen). Protein solutions contained 50% glycerol and were stored at −20 °C.

HldE-K and Ribokinase Assays. The assay buffer "AB" contained 50 mM Hepes, pH 7.5, 1 mM $MnCl_2$, 25 mM KCl, 0.012% Triton-X100, 1 mM dithiothreitol (DTT), and 0.1 μM myelin basic protein (MBP). The following components were added to each well of a white polystyrene Costar plate up to a final volume of 30 μL: 10 μL of a inhibitor dissolved in DMSO/water, 50/50, and 20 μL of *E. coli* HldE in AB. After 30 min of preincubation at room temperature, 30 μL of substrate mix in AB was added to each well to a final volume of 60 μL. This reaction mixture was then composed of 3 nM HldE, 0.2 μM β-heptose 7-phosphate (H7P, custom synthesis) unless otherwise stated, and 0.2 μM ATP unless otherwise stated (Sigma) in AB. After 30 min of incubation at room temperature, 200 μL of revelation mix was added to each well to a final volume of 260 μL, including the following constituents at respective final concentrations: 5000 light units/mL luciferase (Sigma), 30 μM D-luciferin (Sigma), and 100 μM *N*-acetylcysteamine (Aldrich). Luminescence intensity was immediately measured on Luminoskan (Thermofischer) and converted into percentage inhibition. For IC_{50} determinations, each inhibitor was tested at 6−10 different concentrations, and the resulting inhibition data were fitted to a classical Langmuir equilibrium model using XLFIT (IDBS). The same procedure was applied to HldE of *K. pneumoniae*, *N. meningitidis*, and *S. marcescens* at 20, 20, and 10 nM, respectively. The ribokinase assay was basically identical to the HldE-K assay except for the following: H7P was replaced by D-ribose (3 μM); HldE was replaced by ribokinase of *E. coli* (0.6 nM); the concentration of ATP was 3 μM instead of 0.2 μM.

Bacterial Sensitization to Erythromycin. All chemicals were from Sigma unless otherwise stated. From early to log phase preculture, bacterial suspension was prepared in ca-MHB (Becton-Dickinson) to obtain a final inoculum of 5×10^5 CFU/mL. Strains were *E. coli* K12 MG1655 Δ-*acrAB*-Δ*tolc*, *E. coli* K1 (018:K1:H7) wild type, Δ*tolc*, and Δ*hldE*. Each strain was grown in two conditions, one excluding erythromycin and one including erythromycin at a concentration of 1, 8, and 1 μg/mL, respectively. The MIC of the compounds being tested was determined against these strains. Growth was visually inspected in polystyrene 96-well microplates containing serial dilutions of compounds in 2% DMSO after overnight incubation at 35 °C. Each well has a final volume of 100 μL.

HepG2 Cytotoxicity. HepG2 cells (LGC Promochem, ref HB-8065) in EMEM medium supplemented with fetal bovine serum (10%), ampicillin (100 μg/mL), and streptomycin (100 μg/mL) were plated on cell culture plates (Costar 3596, 2×10^4 cells/well) and incubated overnight at 37 °C in 5% CO_2. The culture medium was then aspirated and replaced by supplemented EMEM (210 μL including 2% DMSO) containing dilutions of compounds. Plates were incubated overnight at 37 °C in 5% CO_2. Cell viability was determined by the Celltiter Aqueous One cell proliferation assay (G3581-80, Promega) according to the manufacturer's recommendations, using a Multiskan absorption reader (490 nm).

Inhibition of *E. coli* LPS Biosynthesis. The compounds being tested were prepared in deionized water/DMSO (50/50) solutions, and 25 μL of each solution was added to a sterile culture microtube. The strains used in this study were *E. coli* K12 Δ-*acrAB*, Δ-*tolC* and *E. coli* K1 (018:K1:H7) wild type or Δ*tolc*. The bacteria were isolated on tryptic soy agar (TSA) overnight. Isolated colonies were cultured in 10 mL of Luria−Bertani (LB) medium at 37 °C to an optical density of typically 0.15. These exponentially growing bacteria were finally diluted to 5×10^5 CFU/mL, and 225 μL of each diluted culture was added to each tube for incubation with the compound at 37 °C for approximately 5 h, to an optical density of 0.2−0.4.

LPS Extraction. Bacterial cultures were normalized by optical densities, pelleted, and washed with 1 mL of phosphate buffered saline (PBS). The pellets were then denatured for 10 min at 95−100 °C in 50 μL of 0.2% sodium dodecyl sulfate (SDS), 1% β-mercaptoethanol, 36% glycerol, 30 mM Tris, pH 7.4, and 0.001% bromophenol blue. Samples were cooled to room temperature, supplemented with 1.5 μL of proteinase K at 20 mg/mL, incubated for 1 h at 55 °C, and centrifuged for 30 min at 13 000 rpm at 25 °C. The resulting supernatant, which contained LPS, was finally analyzed by SDS−PAGE.

LPS electrophoresis. Polyacrylamide gels (16% and 4% acrylamide for separation and concentration, respectively) were prepared, loaded with 8 μL of each LPS extract, and migrated.

Silver Staining. Gels were incubated overnight in 5% acetic acid/40% ethanol/deionized water, treated with 1% periodic acid/5% acetic acid for 15 min, washed with deionized water for 10 min for four times, and finally incubated for 18 min in the dark with a silver nitrate solution composed of 56 mL of 0.1 N NaOH, 4 mL of 33% ammoniac, 45 mL of 5% $AgNO_3$ (Tsai and Frasch), and 195 mL of deionized water. Gels were then washed extensively with deionized water for 30 min and incubated for 10−15 min (up to LPS band apparition) in a revelation mix composed of 300 mL of deionized water, 300 μL of 36.5% formaldehyde (Fluka), and 100 μL of 2.3 M citric acid. The revelation was stopped by incubating the gels with 10% acetic acid for 5 min. Gels were finally washed with deionized water, numerized with a Samsung PL51 camera, and analyzed by the ImageJ software. The percentage inhibition of LPS heptosylation was defined as the relative area of the Re-LPS band compared to the total area of the Re-LPS and core-LPS bands.

Sensitization to Killing by Complement. The Gram-negative bacterial strain *E. coli* K12 Δ-*acrAB*, Δ-*tolC* was grown on Müller Hinton agar (MHA) overnight at 35 °C. Five well isolated colonies from overnight agar growth were then added to 10 mL of cation-adjusted Müller−Hinton broth (MH2) and incubated at 35 °C with constant shaking for 2 h to reach the exponential phase. The suspension was then diluted to obtain an inoculum of 1.5×10^4 CFU/mL. Viable counts were obtained by plating 10- to 1000-fold dilutions of the suspension on MHA. A solution of decomplemented fetal bovine serum (dFBS) was prepared by heating the normal FBS at 56 °C for 30 min. Dilutions of each compound being tested were prepared in DMSO/water 20/80 in polypropylene plates. The following components were added on a sterile polystyrene culture plate to a final volume of 100 μL: 5 μL of a compound dilution in 20% DMSO, 30 μL of FBS (30% final) or dFBS (30% final) or MH2 (0% FBS), 65 μL of bacterial suspension at 1.5×10^4 CFU/mL (final inoculum of 1×10^4 CFU/mL). After incubation for 18−22h at 35 °C, the MIC of the compound in the presence of FBS 30%, dFBS 30%, and FBS 0% was determined by visual inspection of bacterial pellets.

dx.doi.org/10.1021/jm301499r | J. Med. Chem. 2013, 56, 1418−1430

General Experimental. All reactions were carried out under inert (nitrogen or argon) atmosphere unless indicated otherwise. Reagents and solvents were obtained from commercial sources and were used without further purification. Celite is a filter aid composed of diatomaceous silica and is a registered trademark of Celite Corporation. Analtech silica gel GF and E. Merck silica gel 60 F-254 thin layer plates were used for thin layer chromatography. Flash chromatography was carried out on Flashsmart Pack cartridge irregular silica 40−60 μm or spherical silica 20−40 μm. Preparative thin layer chromatography was carried out on Analtech silica gel GF 1000 μm, 20 cm × 20 cm. Yields refer to purified products and are not optimized. All new compounds gave satisfactory analytical data. ^{1}H NMR spectra were recorded at 300 or 400 MHz on a Brüker instrument, and chemical shifts are reported in parts per million (δ) downfield from the internal standard tetramethylsilane. Mass spectra were obtained using electrospray (ESI) ionization techniques on an Agilent 1100 series LCMS. HPLC (analytical and preparative) was performed on an Agilent 1100 HPLC instrument with diode array detection. Preparative HPLC was performed at 0.7 mL/min on a Thermo Electron, Hypersil BDS C-18 column (250 mm × 4.6 mm, 5 μm) using a gradient of acetonitrile and water with 0.1% TFA (50% in acetonitrile to 100% and then back to 50%). The tested compounds were determined to be >95% pure via HPLC.

■ ASSOCIATED CONTENT

Supporting Information

Synthetic procedures and spectroscopic details for all final compounds. This material is available free of charge via the Internet at http://pubs.acs.org.

■ AUTHOR INFORMATION

Corresponding Author

*Phone: +33-157140522. Fax: +33-157140524. E-mail: vincent.gerusz@mutabilis.fr.

Present Addresses

[‖]Galapagos, 102 Avenue Gaston Roussel, 93230 Romainville, France.

[⊥]GlaxoSmithKline, 25-27 Avenue du Québec, 91951 Les Ulis, France.

[#]ESE Conseil, 66 Boulevard Senard, 92210 Saint Cloud, France.

[∞]Alderys, 86 Rue de Paris, 91400 Orsay, France.

Notes

The authors declare no competing financial interest.

■ ACKNOWLEDGMENTS

We are grateful to Roowin and Syngene for building block syntheses, as well as to Dr. François Bellamy, Prof. Xavier Nassif, and Dr. Patrice Renaut for stimulating discussions on these topics.

■ REFERENCES

(1) Escaich, S. Novel agents to inhibit microbial virulence and pathogenicity. *Expert Opin. Ther. Pat.* **2010**, *20*, 1401−1418.

(2) Cegelski, L.; Marshall, G. R.; Eldridge, G. R.; Hultgren, S. J. The biology and future prospects of antivirulence therapies. *Nat. Rev. Microbiol.* **2008**, *6*, 17−27.

(3) Gronow, S.; Brade, H. Lipopolysaccharide biosynthesis: which steps do bacteria need to survive? *J. Endotoxin Res.* **2001**, *7*, 3−23.

(4) Coleman, W. G., Jr.; Leive, L. Two mutations which affect the barrier function of the *Escherichia coli* K-12 outer membrane. *J. Bacteriol.* **1979**, *139*, 899−910.

(5) Kneidinger, B.; Marolda, C.; Graninger, M.; Zamyatina, A.; McArthur, F.; Kosma, P.; Valvano, M. A.; Messner, P. Biosynthesis pathway of ADP-L-glycero-β-D-manno-heptose in *Escherichia coli*. *J. Bacteriol.* **2002**, *184*, 363−369.

(6) Alekshun, M. N.; Levy, S. B. Targeting virulence to prevent infection: to kill or not to kill? *Drug Discovery Today: Ther. Strategies* **2004**, *1* (4), 483−489.

(7) McArthur, F.; Andersson, C. E.; Loutet, S.; Mowbray, S. L.; Valvano, M. A. Functional analysis of the glycero-manno-heptose 7-phosphate kinase domain from the bifunctional HldE protein, which is involved in ADP-L-glycero-D-manno-heptose biosynthesis. *J. Bacteriol.* **2005**, *187*, 5292−5300.

(8) Caroff, M.; Karibian, D. Structure of bacterial lipopolysaccharides. *Carbohydr. Res.* **2003**, *338*, 2431−2447.

(9) De Leon, G. P.; Elowe, N. H.; Koteva, K. P.; Valvano, M. A.; Wright, G. D. An in vitro screen of bacterial lipopolysaccharide biosynthetic enzymes identifies an inhibitor of ADP-heptose biosynthesis. *Chem. Biol.* **2006**, *13*, 437−441.

(10) Desroy, N.; Moreau, F.; Briet, S.; Fralliec, G. L.; Floquet, S.; Durant, L.; Vongsouthi, V.; Gerusz, V.; Denis, A.; Escaich, S. Towards Gram-negative antivirulence drugs: new inhibitors of HldE kinase. *Bioorg. Med. Chem.* **2009**, *17*, 1276−1289.

(11) Durka, M.; Tikad, A.; Périon, R.; Bosco, M.; Andaloussi, M.; Floquet, S.; Malacain, E.; Moreau, F.; Oxoby, M.; Gerusz, V.; Vincent, S. P. Systematic synthesis of inhibitors of the two first enzymes of the bacterial heptose biosynthetic pathway: towards antivirulence molecules targeting lipopolysaccharide biosynthesis. *Chem.—Eur. J.* **2011**, *17*, 11305−11313.

(12) Takagi, K.; Iwachido, T.; Hayama, N. Palladium(0)-catalyzed synthesis of 2-alkylbenzothiazoles by a novel thiation of 1-amino-2-iodoarenes with thioamides. *Chem. Lett.* **1987**, *16*, 839−840.

(13) Limanto, J.; Desmond, R. A.; Gauthier, D. R.; Devine, P. N.; Reamer, R. A.; Volante, R. P. A regioselective approach to 5-substituted-3-amino-1,2,4-triazines. *Org. Lett.* **2003**, *5*, 2271−2274.

(14) Oliveira, C.; Vongsouthi, V.; Moreau, F.; Denis, A.; Escaich, S.; Gerusz, V.; Desroy, N. New 1,2,4-Triazine Derivatives and Biological Applications Thereof. WO 2010001220, 2010.

(15) Russell, M. G. N.; Carling, R. W.; Street, L. J.; Hallett, D. J.; Goodacre, S.; Mezzogori, E.; Reader, M.; Cook, S. M.; Bromidge, F. A.; Newman, R.; Smith, A. J.; Wafford, K. A.; Marshall, G. R.; Reynolds, D. S.; Dias, R.; Ferris, P.; Stanley, J.; Lincoln, R.; Tye, S. J.; Sheppard, W. F. A.; Sohal, B.; Pike, A.; Dominguez, M.; Atack, J. R.; Castro, J. L. Discovery of imidazo[1,2-*b*][1,2,4]triazines as GABAA α2/3 subtype selective agonists for the treatment of anxiety. *J. Med. Chem.* **2006**, *49*, 1235−1238.

(16) Grundmann, C.; Schroeder, H.; Rätz, R. New 1,2,4-triazine derivatives. *J. Org. Chem.* **1958**, *23*, 1522−1524.

(17) Kusumoto, T.; Sato, K.-i.; Hiyama, T.; Takehara, S.; Ito, K. Synthesis and electro-optical properties of dihydrobenzofurans and dihydrofuropyridines as chiral dopants for ferroelectric liquid crystals. *Chem. Lett.* **1995**, *24*, 537−538.

(18) Catalan, J.; Del Valle, J. C.; Claramunt, R. M.; Maria, M. D. S.; Bobosik, V.; Mocelo, R.; Elguero, J. Toward the photostability mechanism of intramolecular hydrogen bond systems. 4. 3(5)-(1′-Hydroxy-2′-naphthyl)pyrazoles and 3(5)-(2′-hydroxy-1′-naphthyl)-pyrazoles. *J. Org. Chem.* **1995**, *60*, 3427−3439.

(19) Lee, T.-W.; Verhey, T. B.; Antiperovitch, P. A.; Atamanyuk, D.; Desroy, N.; Oliveira, C.; Gerusz, V.; Malacain, E.; Loutet, S. A.; Hamad, M.; Stanetty, C.; Andres, S. N.; Sugiman-Marangos, S.; Kosma, P.; Valvano, M. A.; Moreau, F.; Junop, M. S. Structure, function and inhibition of D-glycero-β-D-manno-heptose 7-phosphate kinase (HldA) from *Burkholderia cenocepacia*: insights for design of antivirulence drugs or antibiotic adjuvants targeting LPS biosynthesis in gram-negative bacteria. *J. Med. Chem.* [Online early access]. DOI: 10.1021/jm301483h. Published Dec 20, **2012**.

(20) McGovern, S. L.; Helfand, B. T.; Feng, B.; Shoichet, B. K. A specific mechanism of nonspecific inhibition. *J. Med. Chem.* **2003**, *46*, 4265−4272.

(21) Imai, Y. N.; Inoue, Y.; Nakanishi, I.; Kitaura, K. Cl−π interactions in protein−ligand complexes. *Protein Sci.* **2008**, *17*, 1129−1137.

(22) Elkins, C. A.; Nikaido, H. 3D structure of AcrAB: the archetypal multidrug efflux transporter of *E. coli* likely captures substrates from periplasm. *Drug Resist. Updates* **2003**, *6*, 9−13.
(23) Atamanyuk, D.; Faivre, F.; Oxoby, M.; Ledoussal, B.; Drocourt, E.; Moreau, F.; Gerusz, V. Vectorization efforts to increase Gram-negative intracellular drug concentration: a case study on HldE-K inhibitors. *J. Med. Chem.*, submitted.